REPORT DOCUMENTATION PAGE

AFRL-SR-AR-TR-05-

0416

1. REPORT DATE *(DD-MM-YYYY)* 20062005	2. REPORT TYPE Final Report		3. DATES COVERED *(From - To)* 1 Sep 2004 - 31 May 2005
4. TITLE AND SUBTITLE MEMS Colloid Thruster Array		**5a. CONTRACT NUMBER**	
		5b. GRANT NUMBER FA9550-04-c-0067	
		5c. PROGRAM ELEMENT NUMBER	
6. AUTHOR(S) Mr James Nabity		**5d. PROJECT NUMBER**	
		5e. TASK NUMBER	
		5f. WORK UNIT NUMBER	
7. PERFORMING ORGANIZATION NAME(S) AND ADDRESS(ES) TDA Research, Inc 12345 W. 52nd Avenue Wheat Ridge CO 80033		**8. PERFORMING ORGANIZATION REPORT NUMBER**	
9. SPONSORING/MONITORING AGENCY NAME(S) AND ADDRESS(ES) USAF/AFRL AFOSR 875 North Randolph Street Arlington VA 22203		**10. SPONSOR/MONITOR'S ACRONYM(S)** AFOSR	
		11. SPONSOR/MONITOR'S REPORT NUMBER(S)	

12. DISTRIBUTION/AVAILABILITY STATEMENT

Distribution Statement A. Approved for public release; distribution is unlimited.

13. SUPPLEMENTARY NOTES

14. ABSTRACT
TDA designed a single MEMS colloid emitter that can be readily extended to a multi-emitter array. The annular electrodes proposed by TDA and UC-Boulder have high local electric field strength at the nozzle to reduce the voltage needed to activate the electrospray. They also designed a fluidic valve to passively meter flow to each emitter in the array. Detailed micro fabrication process recipes were developed and proven by actually building single emitters. A laboratory test rig has been built, validation tests were conducted using a conventional colloid capillary emitter and tests were attempted using a single MEMS colloid emitter. o Annular emitter electrodes - The annular emitter electrode design doubles the electric field strength in comparison to a full base electrode and thus, lowers the voltage needed to activate the electrospray. It can be micro machined using lithography and vapor deposition processes. o High voltage dielectrics - Teflon films will be used during colloid emitter development to reduce risk. In a parallel task, we will develop and evaluate high quality sputtered silicon dioxide layers based on recent work at the University of Colorado MRTL. Using their equipment and sputter process we can create layers up to 10 pm thick; more than enough for high voltage actuation to 5 kV.

15. SUBJECT TERMS

16. SECURITY CLASSIFICATION OF:			17. LIMITATION OF ABSTRACT	18. NUMBER OF PAGES	19a. NAME OF RESPONSIBLE PERSON
a. REPORT	b. ABSTRACT	c. THIS PAGE			
U	U	U	UU	32	19b. TELEPHONE NUMBER *(Include area code)*

Standard Form 298 (Rev. 8/98)
Prescribed by ANSI Std. Z39.18

DUPLICATE

Phase I Final Report

June 2005

Project Title: MEMS Colloid Thruster Array

Contractor: TDA Research, Inc.
12345 W. 52nd Avenue
Wheat Ridge, CO 80033
(303) 422-7819
(303) 422-7763 FAX

**Principal
Investigator:**   James Nabity
(303) 940-2313
nabity@tda.com

**Contract/Purchase
Order Number**   FA9550-04-C-0067

Contracting Officer:
Ms. Joyce Burch
USAF, AFRL
AF Office of Scientific Research
4015 Wilson Blvd, Room 713
Arlington, VA 22203-1954

Program Manager:
Dr. Mitat Birkan
AFOSR/NA
4015 Wilson Blvd, Room 713
Arlington, VA 22203-1954

Reporting Period: Sep 1, 2004 – May 31, 2005

Date of Report: June 20, 2005

SBIR Rights Notice (252.227-7018 dated June 1995)

Contract No: FA9550-04-C-0067
Contractor Name: TDA Research, Inc
Address: 12345 W 52nd Ave, Wheat Ridge, CO 80033
Expiration of SBIR Data Rights Period: May 31, 2010

For a period of five (5) years after completion of the project from which the data was generated, the Government's rights to use, modify, reproduce, release, perform, display, or disclose any technical data or computer software contained in this report are restricted as provided in paragraph (b)(4) of the Rights in Noncommercial Technical Data and Computer Software Small Business Innovative Research (SBIR) Program clause contained in the above-identified contract [DFARS 252.227-7018 (Jun. 1995)]. No restrictions apply after expiration of that period. Any reproduction of technical data, computer software, or portions thereof marked as SBIR data must also reproduce those markings and this legend.

Executive Summary

Colloid thruster technology continues to be attractive for spacecraft propulsion, especially since the specific impulse can be many times greater than even the best bi-propellant chemical rocket. However, the technology was abandoned in the 1970's due to low propellant charge-to-mass ratios, which lead to excessively high voltages and a large inert mass fraction. The recent advent of highly conductive propellants coupled with microelectromechanical systems (MEMS) technology created renewed interest in colloid thrusters for micro- and nano-satellite applications. Colloid thruster arrays can produce relatively large thrust levels, while maintaining the ability to deliver a small impulse bit. However, difficulties in fabrication and assembly, the need for high voltage addressing and thruster operability issues have hindered full development of the concept at the micro-scale. TDA Research, Inc., teamed with personnel from the University of Colorado at Boulder (hereafter UC-Boulder) and Aerojet-Redmond, proposed to build MEMS colloid thruster arrays. In Phase I we designed a single MEMS colloid emitter that overcame these technological barriers. We doubled the electric field strength at the emitter nozzle over that achieved by previous investigators through electrode design, so that Taylor cone formation should be able to be initiated at much lower voltage and yet still attain high propulsive efficiency. We developed a micro fabrication process recipe to build single emitters (one shown in Figure 1) that can easily be extended to build two-dimensional arrays. We also designed a fluidic valve to balance the propellant flow to each emitter in the array. Finally, we used our apparatus to demonstrate electrospray formation from a capillary emitter as shown in Figure 2. In Phase II we will improve upon our MEMS design, implement the fluidic valves, simplify the micro fabrication process recipe, increase the array packaging density, and demonstrate thrust modulation from addressable 2D colloid thruster arrays.
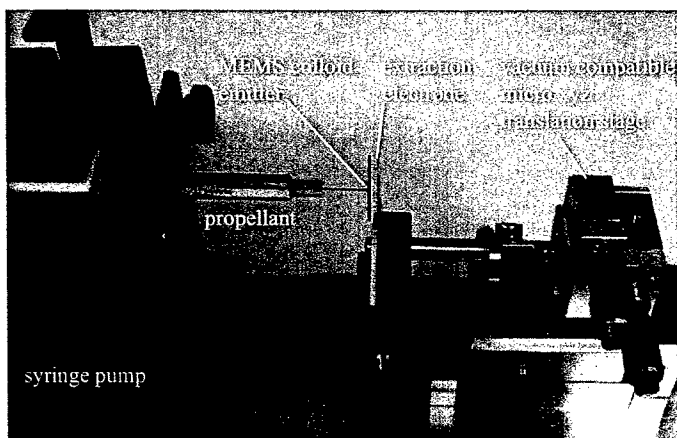
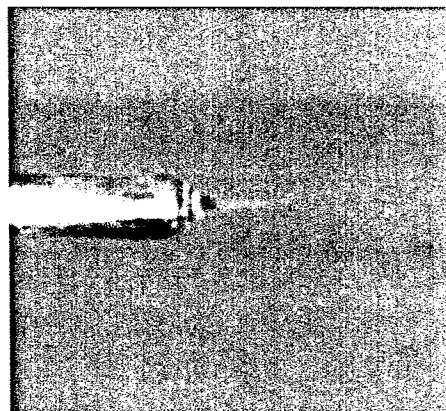Figure 1. Single MEMS colloid emitter on laboratory test stand.

Figure 2. Electrospray from capillary emitter.

Table of Contents

List of Figures

List of Tables

None.

1. Nomenclature

f   relative electric field strength
g   gravitational acceleration
I_{sp} specific impulse
K   propellant electrical conductivity
m   mass
$\dot{m}$ mass flow rate
MEMS microelectromechanical systems or structures
P   gauge pressure relative to ambient
q   electrical charge
Q   propellant flow rate
r   radius from the emitter centerline
$\dot{r}$ etch rate
SOI   silicon-on-insulator
T   thrust, temperature
u   velocity
Δv change in velocity
V   voltage

ε_o permittivity = 8.85×10^{-6} pF/um
ε dielectric constant (propellant or dielectric material)
γ surface tension
ρ density

<u>subscripts</u>
e   exit
o   initial

2. Project Summary

Colloid thruster technology continues to be attractive for spacecraft propulsion, since the specific impulse can be many times greater than even the best bi-propellant chemical rocket. However, the technology was abandoned in the 1970's due to low charge-to-mass ratios, which lead to excessively high voltages and a large inert mass fraction. The recent advent of highly conductive propellants coupled with microelectromechanical systems (MEMS) technology has created renewed interest in colloid thrusters for micro- and nano-satellite applications. Colloid thruster arrays can produce relatively large thrust levels, while maintaining the ability to deliver a small impulse bit. However, difficulties in fabrication and assembly, the need for high voltage addressing and thruster operability issues have hindered full development of the concept at the micro-scale. TDA Research, Inc., teamed with personnel from the University of Colorado at Boulder (hereafter UC-Boulder), proposed to build MEMS colloid thrusters. We overcame these barriers using new electrode and flow control designs developed under this Phase I contract, and by taking advantage of wafer level microfabrication and assembly processes that we had previously developed during execution of ONR Phase II SBIR Liquid Fuel Atomizer (contract # N00014-01-C-0457 under Technical Monitor Dr. Chris Brophy, May 2002 - Nov 2004).

Micro-satellites impose a significant propulsion challenge because extremely small impulse bits (I_{bit}) are required for precise attitude control, whereas slew rate and orbital requirements demand much larger thrust levels; in fact more than 1000X greater. One solution to this dilemma is to use MEMS technology to build thrusters sized for tracking thrust and impulse maneuvers, and gang many of them together to meet slew rate and orbital change requirements. Microfabrication processes readily permit multiple replications on a single chip or wafer, but colloid thruster density will largely be determined by the design and layout of the high voltage microelectronics for actuation and the microfluidic components needed to control propellant flow. Our current thruster array layout indicates that 100 thrusters can be built on a single 1cm x 1cm chip assembly, but there is plenty of room for improvement. Additional process optimization to use thinner wafers can reduce the center-center spacing to as small as 200 μm. Thus, we could potentially batch fabricate up to 2,500 thrusters on the same 1cm x 1cm chip.

Practical microfabrication strategies are needed to create dense two-dimensional arrays of individually addressable emitters incorporating high voltage electrodes. High voltage actuation is highly desirable, since specific impulse increases with voltage. Further, each emitter must be able to produce uniform thrust, which is a key challenge in thruster array development. Research has shown the tendency for most emitters in an array to run dry, while only one or two emitters actually produce thrust; this severely reduced the thrust-to-weight ratio of previous thruster arrays.

In the proposed effort TDA and UC-Boulder built upon the work of Paine, et al. [1-2] (Figure 3) to construct colloid thrusters at the wafer level. In their concept a manifold supplies the propellant to the nozzle. One electrode is formed from the semi-conducting silicon wafer and the other from a vapor deposited metal layer. A silicon dioxide insulator separates the charged electrodes. Further, in this design the electrodes are recessed relative to the nozzle to avoid voltage breakdown by surface flashover. Their work shows promise, since they have fabricated 2D colloid thruster arrays capable of high voltage actuation using standard MEMS microfabrication processes. However, fully functional emitters have yet to be demonstrated and their design does not address the issue of uniform thrust production. Therefore, in Phase I we

2

improved the electric field strength through electrode design, developed micro fabrication process recipes and evaluated novel flow control strategies to ensure uniform propellant feed to all emitters.
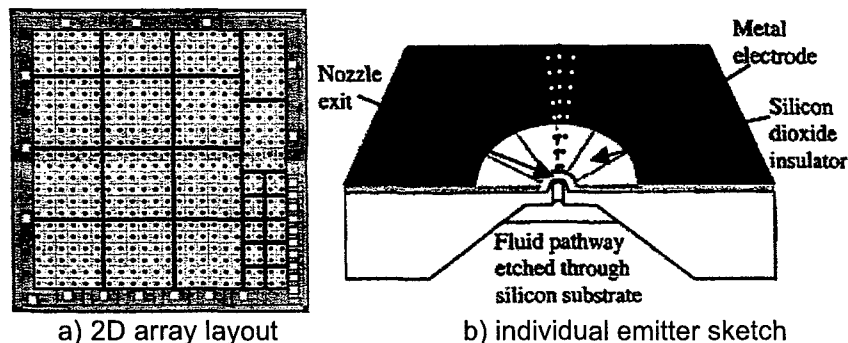

a) 2D array layout

b) individual emitter sketch

Figure 3. Wafer level 2D colloid thruster array design of Paine, et al. [1-2].

TDA and UC-Boulder personnel have teamed on three research projects to analyze, develop and build MEMS atomizers using high voltage electrostatic actuation. [3,4,5] Many of the lessons learned and fabrication methods that we have developed are directly applicable to colloid thrusters. In the course of our research we have applied multi-physics numerical codes to fully coupled electrostatic-structural-microfluidic problems [3] very much like the colloid thruster. Thus, we have the tools to analyze and layout colloid thruster designs. In addition, we have extensive experience in the lithography, etch and vapor deposition processes that are needed to fabricate MEMS based colloid thruster arrays.

In Phase I we designed a single MEMS colloid emitter with a local electric field strength of nearly that attained with a conventional colloid capillary. Thus, Taylor cone formation should be initiated at much lower voltage and still attain high propulsive efficiency. We developed a micro fabrication process recipe to build single emitters (one shown in Figure 4) that can easily be extended to build two-dimensional arrays. We also designed a fluidic valve to balance the propellant flow to each emitter in the array. Finally, we showed that our laboratory test rig could control the ionic liquid flow delivery and apply the needed voltage potential to initiate Taylor cone formation from a conventional capillary emitter.
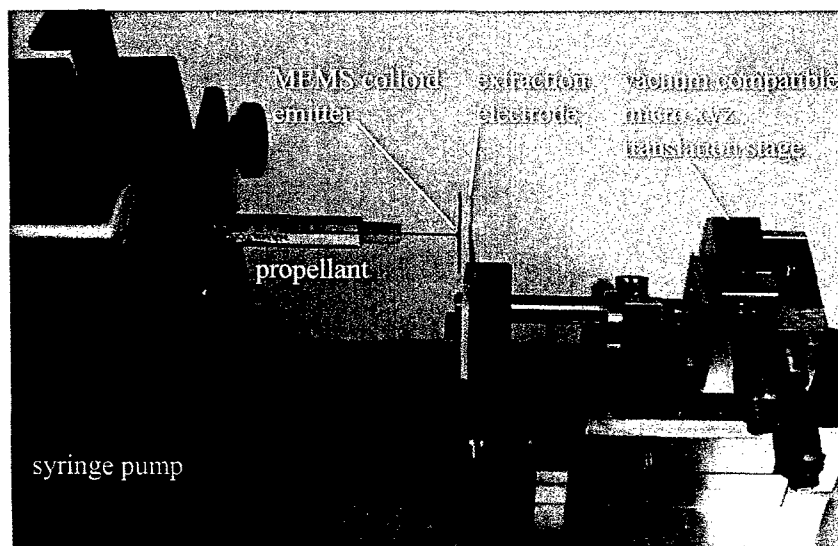

Figure 4. Single MEMS colloid emitter on laboratory test stand.

3. Objectives

In Phase I we met our objective to show through analyses and testing that the proposed MEMS colloid thruster array could be designed and fabricated. A key objective was to develop and demonstrate the microfabrication processes needed to build two-dimensional colloid thruster planar arrays from silicon wafers. We fabricated single emitter prototypes for electrospray tests and completed a preliminary layout of a two-dimensional thruster array.

The technical questions that we answered in Phase I were:
1. What silicon micromachining processes and processing order will be best suited for colloid thruster array fabrication?
2. What emitter array density may be achieved?
3. What flow control authority will be required to assure uniform fueling of the emitters?
4. What electrode design can enable individual addressing with high voltage actuation?

To answer these we defined the process recipe needed to build single colloid emitters, created a two-dimensional array layout to calculate the packaging density, conducted a numerical study to evaluate flow control passages and simulated electrode designs to improve upon the Paine and Gabriel concept [1-2]. At present we can achieve a packaging density of 100 thrusters / cm^2, but believe that this can be increased by 25X through improved design, thinner wafers and optimized micro fabrication processing. Our annular electrode produces twice the local electric field strength of the Paine and Gabriel full base electrode design and our field strength at the emitter therefore approached that of conventional capillary emitters.

The detailed design, development, fabrication and testing of 2D MEMS colloid thruster arrays will be the focus of Phase II. We will continue our numerical analyses in support of thruster design. In these studies we will determine the effect of nozzle configuration and electrode design on droplet formation. We will explore spacecraft neutralization concepts such as alternate charging. Thruster array assembly and packaging will be evaluated to improve reliability. Laboratory investigations of addressable emitter activation will be conducted to determine the adequacy of our flow control approach to balance the propellant delivery. This will include the testing of two-dimensional emitter arrays to verify thruster performance and thrust modulation. We will consult with Aerojet about microsat system integration issues under an existing confidential disclosure agreement. We expect to demonstrate a fully functional MEMS colloid thruster array by the end of Phase II.

4. Phase I Results

TDA Research and UC-Boulder designed a MEMS colloid emitter, defined microfabrication process recipes to build a single colloid emitter and designed a propellant delivery system. The electrodes are crucial to emitter operation in the cone mode, so UC-Boulder analyzed the electrode design and developed a new geometry to increase the electric field strength at the emitter tip. The geometries were consistent with MEMS fabrication processing (i.e. we can make them). Process recipes were formulated that were used to build emitter chips with etched propellant flow channels and vapor deposited electrodes. We assembled and tested both conventional metal capillary and MEMS colloid emitters. Our laboratory test apparatus was successfully validated by the capillary emitter test, but unfortunately the MEMS emitter failed to function properly since the emitter electrode had been inadvertently blown off during assembly. Compressed gas was used to clear fouled micro passages, but unfortunately this also blew the electrode off the surface. Revisions to the micro fabrication and assembly procedures have been made that should prevent fouling and better protect the microelectronics.

4.1 Overview

Colloidal thruster technology is based on the electrostatic acceleration of small droplets that are generated by feeding a conducting fluid through a small capillary (50 microns is typical, but we can reduce the diameter to a few microns with MEMS fabrication processes). Experiments have shown that best results are achieved when the system is operated in the "cone" mode, which occurs when the volumetric flow rate lies between the limits

$$\frac{\gamma \varepsilon_0 \varepsilon}{\rho K} < Q < (20 \: to \: 30) \cdot \frac{\gamma \varepsilon_0 \varepsilon}{\rho K}$$

where γ is the liquid surface tension, ε_0 is the permittivity of free space, ε is the dielectric constant of the fluid, ρ the density and K the electrical conductivity. Key to the design is determining an electrode pattern layout that can create the needed electric field strength to initiate Taylor cone extraction.

For typical doped propellants with K ~ 1 S/m, the minimum flow rate is about 5×10^{-5} mm^3/sec. In this limit of very low flow rate, the electrostatic field causes a very narrow jet of charged liquid to form at the tip of the cone. The jet then breaks down into fairly monodisperse and small droplets via the classical Rayleigh mechanism. The droplets are subsequently accelerated to high velocities after leaving the nozzle; specific impulses (I_{sp}'s) of a few thousand seconds have been demonstrated [3]. The specific impulse and thrust of a colloidal thruster is given by

$$I_{sp} = \frac{1}{g}\sqrt{2\frac{q}{m}V} \qquad \text{and} \qquad T = \dot{m}u_e = g\dot{m}I_{sp}$$

where q/m is the charge to mass ratio of the droplets. Using doped propellants (i.e. formamide, glycol, imidazolium salts in organic solvents, etc.), charge to mass ratios close to 10,000 C/kg have been achieved. Voltages of several thousand volts are typically used; for example, 5 kV will result in an I_{sp} of 1000.

The colloid thruster technology is attractive for several reasons. Operation in the "cone" mode means that an individual emitter produces very little thrust, about a µN, which is well suited for attitude control of micro and nano satellites. Then, we can replicate hundreds of emitters on a single chip using MEMS fabrication to provide the higher levels of thrust required for large Δv maneuvers; for example, a 1 cm^2 array should produce nearly a mN of thrust.

5

4.2 Colloid Thruster Array Design

Our MEMS colloid thruster was adapted from the work of Paine, et al. [1] and as previously shown in Figure 3. This simple design can be easily fabricated by bulk micromachining a silicon-on-insulator wafer to form the manifold and using reactive-ion-etch to bore the nozzle. Vapor deposited metal forms the extraction electrode. However, their emitters have several drawbacks; first because the extraction and resulting emitter electrodes were only microns apart, the electric field was not well suited to Taylor cone extraction (compare Figure 5a to an ideal configuration shown in Figure 5b), second, the use of a thermally grown silicon dioxide dielectric limited the applied voltage to about 1500V [2], and third, there was no method to control propellant flow to the individual emitters in an array.

Therefore, electrode design was crucial to create the needed electric field strength at the point of Taylor cone extraction. Applying the SIMION code to first solve Laplace's equation for the electric field and then to calculate the droplet trajectories, we found that we could double the electric field strength at the nozzle exit by using small annular electrodes and by increasing the axial distance separating the first extraction electrode from the emitter electrode (Figure 5c).

The increased separation also ensured that adequate voltage could be applied to initiate the Taylor cone extraction without shorting the electrodes, yet we could still easily fabricate our emitter on a double-sided polished wafer as shown in Figure 6.
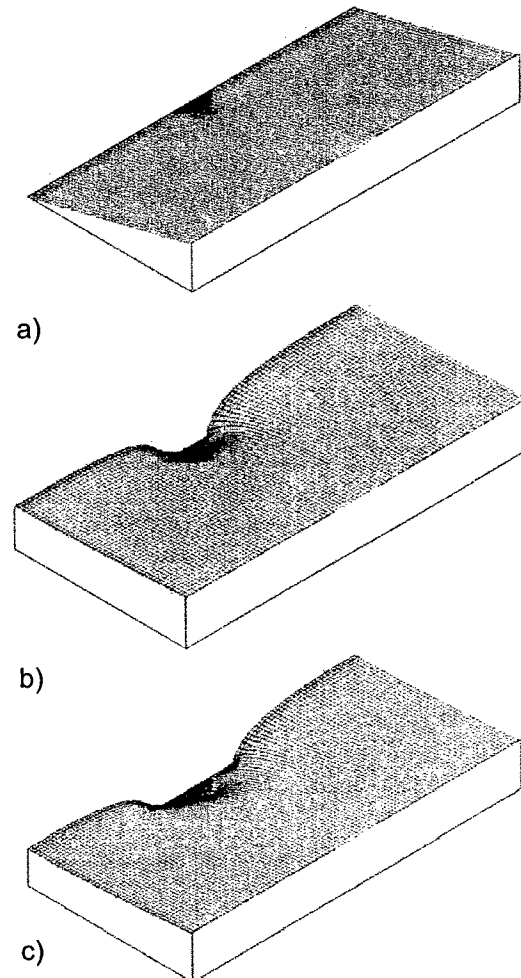
a)

b)

c)

Figure 5. Electric field line sketches: a) non-ideal for a full-base electrode, b) ideal point source electrode, and c) close to ideal small annular electrode.

In Figure 7 we show an exploded view of a single colloid emitter that was built to evaluate our emitter design. A glass capillary fed propellant to the emitter. Applying voltage across the two electrodes will generate the needed electric field strength to initiate Taylor cone extraction and form the electrospray. Our calculations show that electrode separation may need to be as great as hundreds of microns. Thermally grown oxide and sputtered dielectric layers will not provide this separation by themselves, since they are limited to microns thick layers. In addition, an air gap cannot provide adequate breakdown resistance until the gap is more than 600 μm or the ambient pressure reduced to less than 40 mTorr. Therefore, in Phase I we made the extraction and acceleration electrodes from Teflon coated copper foils. Teflon forms a very robust dielectric, which quickly allowed us to build test emitters. The electrode was pierced to permit the spray to pass through. In Phase II, we will replace Teflon with sputtered silicon dioxide

dielectrics. The colloid emitter assembly was bonded to a glass capillary and lastly, insulated wires were bonded to the electrode bond pads to power the device.
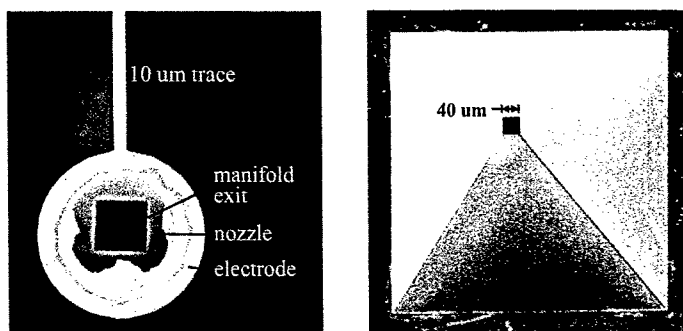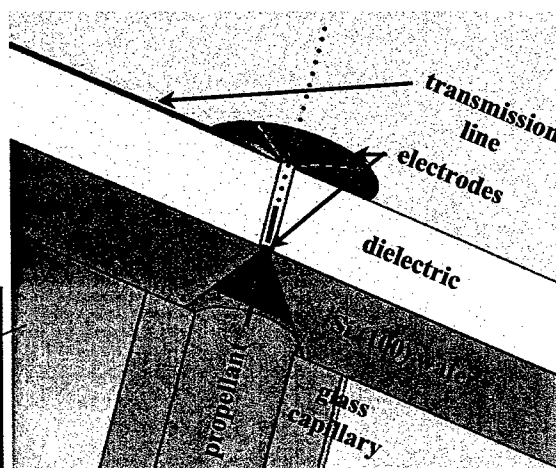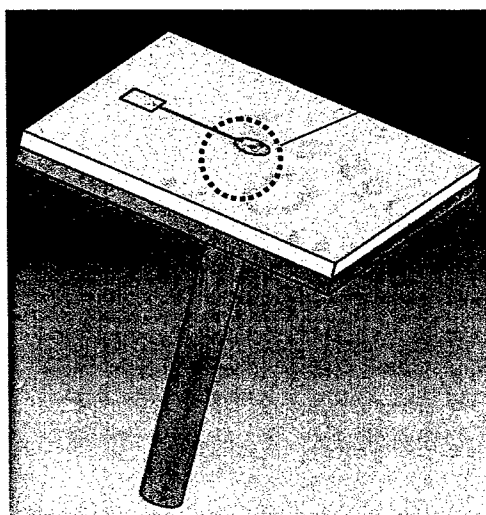

Figure 6. SEM images of a MEMS emitter fabricated by TDA (upper and lower surfaces are shown; a separately fabricated extraction electrode is not shown).

Emitter electrode:	70 um outer dia
	50 um inner dia
Extraction electrode:	1000 um outer dia
	100 um inner dia
Transmission lines:	<10 um wide
Dielectric:	TBD thick
Nozzle:	<50 um dia
	TBD length

Figure 7. TDA / UC-Boulder MEMS colloid emitter design.
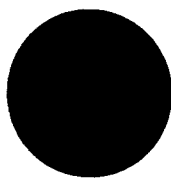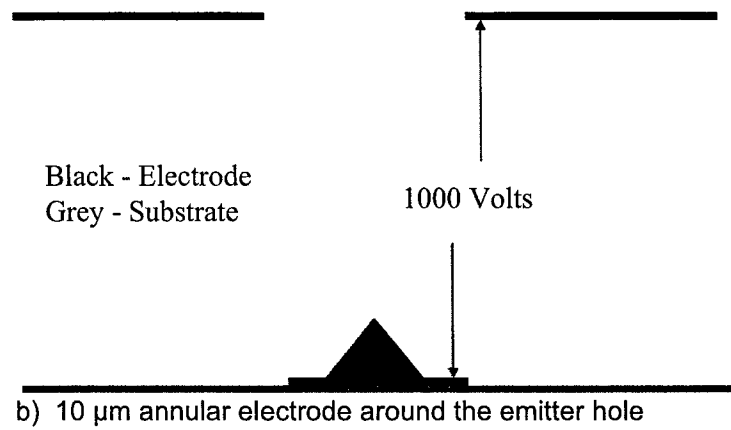
4.2.1 Electrostatic and Droplet Dynamic Modeling

Analyzing the colloid emitter from propellant feed to droplet expulsion requires multi-physics analysis tools not yet available; for example, the Taylor cone extraction and droplet breakup behavior is particularly complex. However, codes are available to solve Laplace's equation for the electric field and then calculate droplet trajectories. Therefore, to model the droplet dynamics once they have been formed we utilized the SIMION program. This program was designed to carry out potential field calculations and then track charged particle motion through the field. Our initial simulations focused on optimizing the electrode configuration within the constraints imposed by micro machining processes.

7

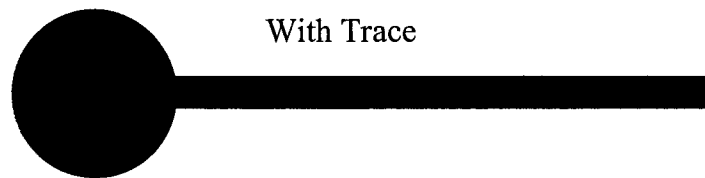In a conventional colloid thruster, the propellant is ejected through a small metal capillary in the presence of a large electric field to create an electrostatic spray. The capillary serves as the emitter electrode, and there is a second electrode (the extractor) placed some distance away. Typically, the emitter is operated in the "cone" mode. In this mode the propellant forms a cone at the exit of the capillary. Because of the field concentration at the tip of the cone, the electric field is very high, causing charge separation in the liquid. This results in a narrow jet (tens of nanometers in diameter) being formed, from which charged droplets are removed and accelerated away from the tip by the electric field. To first order we can assume that the extracted propellant cone is at the same potential as the emitter electrode. Therefore, the cone becomes part of the emitter electrode. The cone and surrounding metal electrode then determine the local electric field.

In the MEMS configuration, the emitter will have to be a hole in the silicon substrate, and the electrode plated onto the substrate upper surface. One goal of our simulations was to determine an electrode configuration that optimized performance. The choices were for the electrode to completely cover the substrate (the simplest to fabricate), or for it to form a small annular region around the hole in the substrate (relatively simple to fabricate). In the latter case it could be electrically connected to the outside circuit by a via through the substrate, which is somewhat more difficult to fabricate, or by a trace electrode off to the side, which is no more difficult than depositing the annulus. These three possibilities are illustrated in Figure 8 and were analyzed using SIMION. Here the cone was modeled as part of the electrode, the extraction electrode was placed 200 μm above the emitter. The findings are summarized as follows:

1. For a full base electrode, the electric field at the tip of the cone was reduced by about 50% as compared to the small annular emitter electrode. Twice the voltage potential would be needed for a full base electrode configuration to create the same field strength at the emitter tip.

Black - Electrode
Grey - Substrate

1000 Volts

a) emitter electrode completely covers the base substrate (analogous to Paine and Gabriel. [1])

Black - Electrode
Grey - Substrate

1000 Volts

b) 10 µm annular electrode around the emitter hole
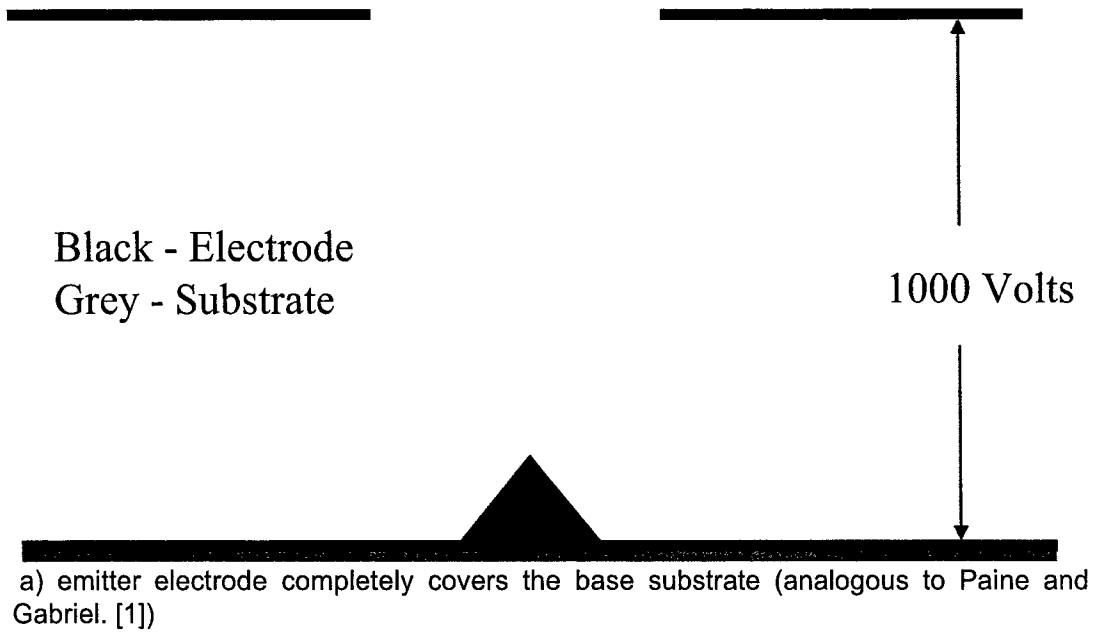
Without Trace

With Trace

c) top view of the annular emitter with via and with trace

Figure 8. Candidate electrode configurations

2. The difference in electric field strength at the tip given a trace or a via was less than 1%. However, with the trace, there was a slight asymmetry in the electric field. Therefore, the droplets tend to drift away from the trace. The effect is small, about 2.5 in 100, and if necessary could easily be corrected with focusing electrodes. Therefore, because of simplicity, the trace configuration is preferred.

3. The velocity to which a charged droplet can be accelerated depends on both the voltage difference between the emitter and the extractor electrodes and the initial kinetic energy (KE) as it separates from the cone. Therefore, for equal initial KE, there is no difference in final droplet velocity between any of the cases. However, the initial KE was a strong function of the electric field at the tip. Furthermore, a minimum field strength must be generated to initiate the droplet formation process. Because of these effects, we wanted the field to be as large as possible for a given applied voltage. Therefore, the small annular electrode with trace or via connection was again preferred.

The potential contours for the case with the 10-μm wide trace of Figure 8c are plotted in Figure 9. As can be seen, the potential field gradients are largest at the tip of the cone.

We also explored a hexagonal pattern emitter layout in which each emitter was equidistant from its neighbors as shown in Figure 10. This staggered center pattern was used to evaluate local emitter-to-emitter influences on the electric field.
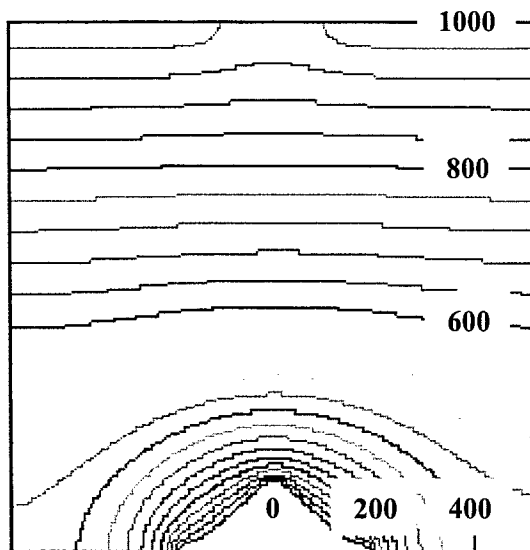

Figure 9. Contour plot of the potential field for the 10-μm wide trace. The plot is for a plane that cuts through the center of the cone with voltage potential varying from 0 volts at the emitter electrode to 1000 volts at the extraction electrode.
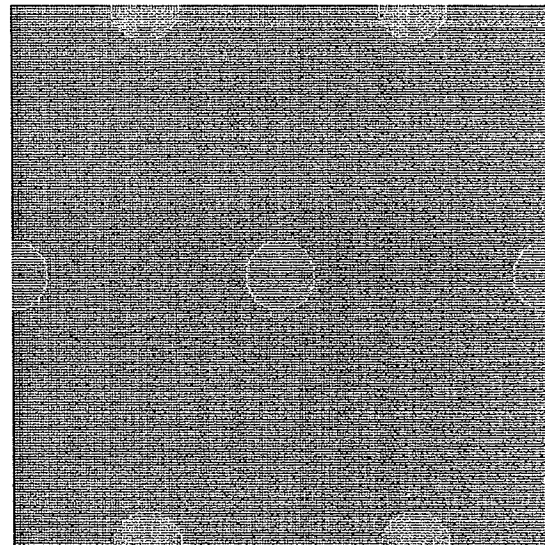

Figure 10. Hexagonal layout of emitters on a planar substrate.

If we assume that the electric field around the axis of the jet is the same as for a conductor, then to a first approximation the potential field behaves as

10

$$V = V_0 \frac{r_0^2}{r^2}$$

Thus, the potential field will drop to a fraction **f** of its value, when $r = \sqrt{\frac{1}{f}} r_0$. As a conservative estimate, we take $r_0 = 25 \mu m$ and f = 0.05, then by about 110 µm from the emitter centerline the field will have dropped to 5% of its maximum value. Figure 11 shows a SIMION simulation for a 250 µm center-to-center spacing, which appears adequate to minimize multi-emitter interactions. At this spacing nearly 2000 emitters could be packaged onto one square centimeter. At this time, the emitter electrode spacing does NOT limit the packaging density that may be achieved.
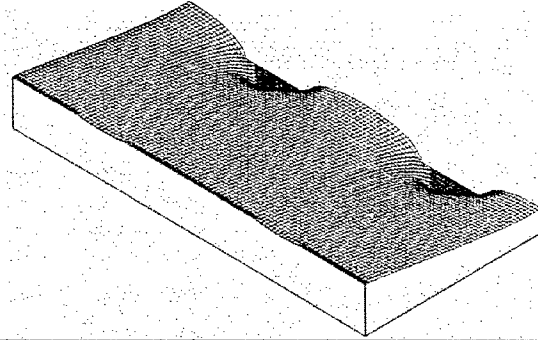

Figure 11. Potential field distribution on the plane intersecting two emitters; 250 µm center-center spacing.

4.2.2 Propellant Flow Control

We believe the most promising approach to flow control will use passive fluidic valves that can be readily surface micromachined. Propellant flow will branch from the manifold to the emitters through flow restrictive passages. An array design is shown in Figure 12. This pattern can be replicated as needed across the chip.

The flow passage must be sized to have sufficient pressure drop to balance the flow to each emitter, yet still be able to pass the needed flow to generate an electrospray. We used FLUENT to numerically simulate simple channels to throttle the flow to the emitter. The channels will be triangular shaped as a result of being KOH etched into <100> silicon. The base was varied from 2 to 50 µm and the two included angles of the isosceles triangle with respect to the <100> plane are 54.7 degrees. The flow channel length was 10X the width. Imposing a symmetry plane through our model reduced the calculation volume.
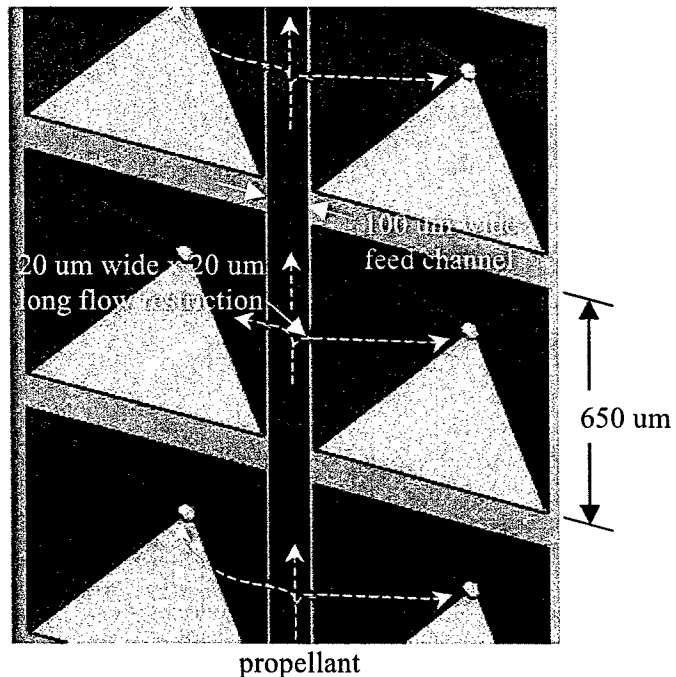

20 um wide x 20 um long flow restriction

100 um wide feed channel

650 um

propellant

Figure 12. Propellant feed system layout.

11

Our results shown in Figure 13 indicate that a flow channel width between 20 and 50 µm will be about right. The pressure drop is substantial in comparison to the outlet pressure drop. In order to improve packaging density we reduced the flow channel length from 10X to 1X the width. Thus, a flow channel with a 20-µm wide base and length were selected. The flow restriction pressure drop was 405 mTorr and the calculated pressure field is shown in Figure 14.
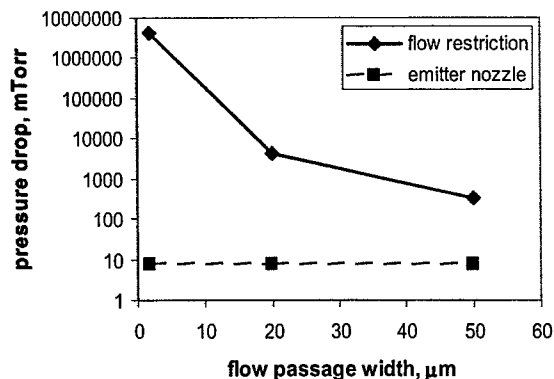

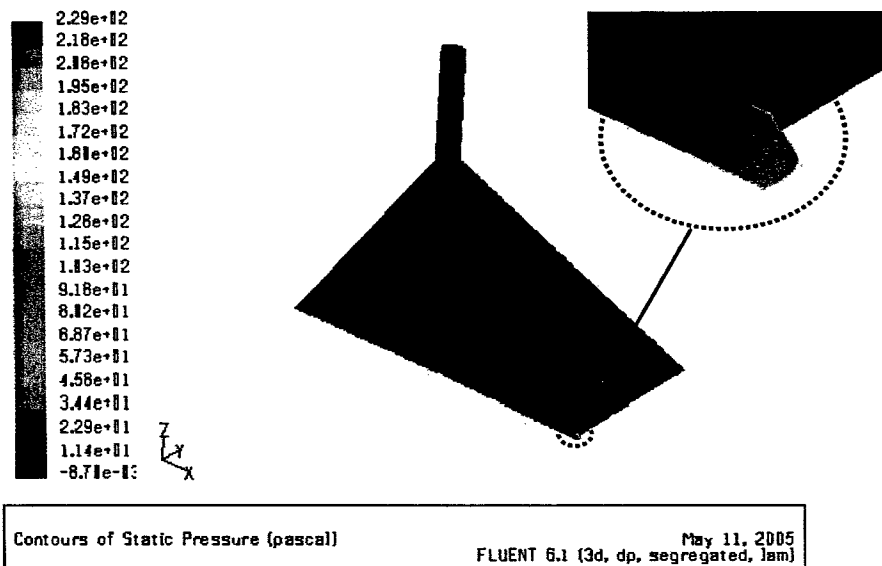Figure 13. Flow restriction results calculated with FLUENT.

Contours of Static Pressure (pascal)   May 11, 2005
FLUENT 6.1 (3d, dp, segregated, lam)

Figure 14. Pressure contours showing flow restriction to balance the flow; a 20-µm wide base with the length equal to the width.

One of our goals in Phase II will be to significantly reduce the volume of the KOH etched pyramid. We expect to accomplish this by utilizing thinner wafers so that the total KOH and RIE etch depth to breach the wafer will be reduced from about 480 µm to 320 µm. In addition, we will vapor deposit thicker mask layers for the RIE etch so that the nozzle may be bored to a greater depth. Utilizing these approaches we expect to reduce the pyramid dimensions from 600 µm to at least 340 µm, which will reduce the total pyramid volume by a factor of five (5).

4.2.3 High Voltage Actuation

A colloid emitter needs large electric field strength from at least 1 V/µm to as much as 10 V/µm to create an electrospray. Yet, thermally grown and sputtered MEMS dielectrics that were available at the time had limited voltage standoff capability, so better dielectrics were needed. The most direct and cost-effective way to solve this dilemma was to implement an existing high voltage dielectric such as Teflon. It will be used until we apply higher voltage micro fabricated dielectrics in Phase II.

4.3 Prototype Fabrication

The fabrication of addressable 2D colloid thruster arrays challenges conventional MEMS processes, but we outline a wafer level fabrication methodology that will be used to build two-dimensional arrays of colloid thrusters. Our emitter array design evolved as we incorporated new analysis and fabrication layout results. All of the fluid flow path features were etched into a single double-sided polished wafer. We propose a second single-sided polished wafer to close the open channels in our multi-emitter design. Referring to the assembly in Figure 15 we first need to pattern and bulk etch the pyramidal chamber that nearly breaches the wafer from the back side, as well as the propellant feed lines and fluidic valves. The nozzles are reactively ion etched from the front side of the wafer to the chamber. In the figure we show individually addressed annular electrodes around each nozzle. Traces are routed to the edges of the array for wire-bonding to a package (not shown in the figure). We used the University of Colorado Microfabrication Research and Teaching Laboratory (MRTL) for process development and fortunately, only a few major process steps were needed to produce our MEMS colloid emitters. We detail these in the following sections.

4.3.1 MEMS Fluidic Flow Paths

Flow path fabrication, such as the propellant manifolding, delivery lines and valves, required a controlled etch of the lithographically patterned silicon wafer to create the desired flowpath features. A photo mask was placed directly on the photoresist-coated silicon wafer using a Karl Suss MJB3 mask aligner. The wafer was exposed to UV light and subsequently etched to pattern the photoresist. The patterned photoresist layer was then transferred to the underlying silicon nitride layer by plasma reactive ion etch. Next, the patterned features were wet etched to the

Figure 15. Emitter assembly sketch.

required depth in a temperature controlled KOH bath. The buffered KOH bath anisotropically etched silicon wafers quickly and with a high degree of resolution to pattern the wafer. The <100> silicon surface was etched at a rate of 20 μm/hr at 70°C.
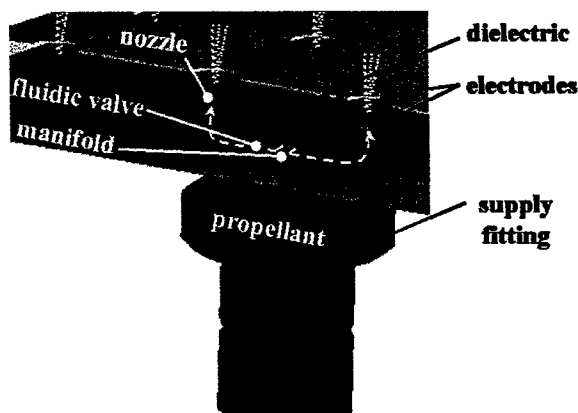
We used reactive ion etch to machine the colloid emitter nozzle orifice. Reactive ion etch (RIE) offers an affordable, rapid and readily available process for micromachining silicon. RIE etches many materials equally well, so it can often be challenging to create large aspect ratio features. However, nickel provided good pattern results to at least 50 μm etch depth in silicon and greater etch depth appears feasible. First, we patterned the wafer with negative photoresist. Then, chromium and nickel were vapor deposited. An acetone bath removed the remaining photoresist and thereby lifted off the unwanted nickel to form the patterned mask for RIE etch. Then, the reactive ion plasma etch preferentially etched the silicon in the vertical direction.

The MRTL has a Plasma-Therm model 540, which was recently modified for SF_6 and SF_6/O_2 plasmas. Much greater etch rates into silicon could be achieved than with the CF_4/O_2 plasma. Processing optimization was conducted and to date we can etch almost 2 μm/min by flowing 5 sccm SF_6 at 80 mTorr pressure with the power level set at 500W.

Propellant chamber process recipe

The following processing details were needed to bulk etch propellant flow passages, such as the pyramidal shaped chamber, feed lines and valves, from the back side of the double-sided polished (DSP) wafer using a silicon nitride mask.

1) Piranha clean the double-sided polished wafer.
2) Vapor deposit silicon nitride.
3) Spin coat hexamethyldisilazane (HMDS) primer for 40 sec at 4000rpm to improve adhesion. Then, spin coat NR7-1500PY negative photoresist (PR) for 40 sec at 4000rpm. Then, pre-bake for 1 minute at 150°C on a vacuum hot plate.
4) Optional step: Pattern the wafer for thick outer edge removal using process steps 6-8 below. A special mask will be required for this purpose. Thus, the remaining PR is flat resulting in improved surface contact and feature resolution for lithography of the MEMS devices.
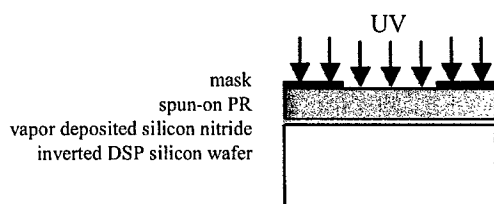
5) UV Lithography: mask align using a Karl Suss MJB3 and expose the wafer to UV light for ~25 to 30 seconds.
6) Post bake at 100°C for 1 minute on a vacuum hot plate.
7) Spray RD6 developer onto the front side of the wafer for 5-6 seconds, while spinning at 800 rpm. Watch for PR to wash off (reddish colors spin off and then wafer looks clear). A second or two of over-development is OK. Apply de-ionized water for 20 sec to quench development and thoroughly rinse the wafer. Spin dry at 3000 rpm.
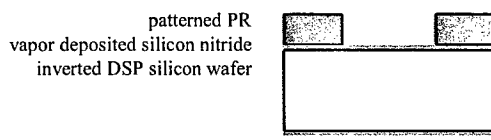
8) Use March oxygen RIE to perform a 'de-scum' process for 10 seconds, which fully cleans the exposed oxide surface. Additional exposure may be required.
9) Use the Plasma-Therm model 540 for 6 min at 150W to CF_4/O_2 plasma reactive ion etch (RIE) through the exposed silicon nitride.
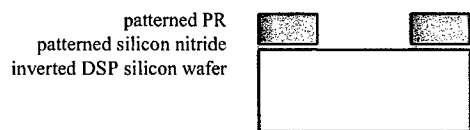
10) Optional step, but a good idea: Strip the PR from the wafer with RR2 to fully expose the patterned silicon nitride layer.
11) KOH etch the wafer to nearly breach the wafer. The etch rate in <100> Si wafer is about 20 μm/hr @ 70°C, so about 24hrs is needed. Rinse 3X with de-ionized water.
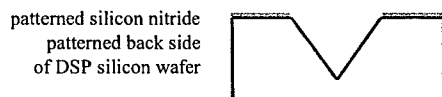

Figure 16. Propellant manifold process recipe: UV lithography with negative PR followed by KOH etch.

In order to make the emitter chamber, a silicon nitride coated DSP silicon wafer was first lithographically patterned (Figure 17a). Then, the pattern was transferred to the silicon nitride via reactive ion etch (Figure 17b). Next, the photoresist was removed and the chip was placed in the KOH bath for 24 hrs. The resultant pyramid-shaped pit nearly breached the silicon chip

a) lithographically patterned photoresist

b) RIE patterned Si_3N_4

c) KOH etched silicon (top view)

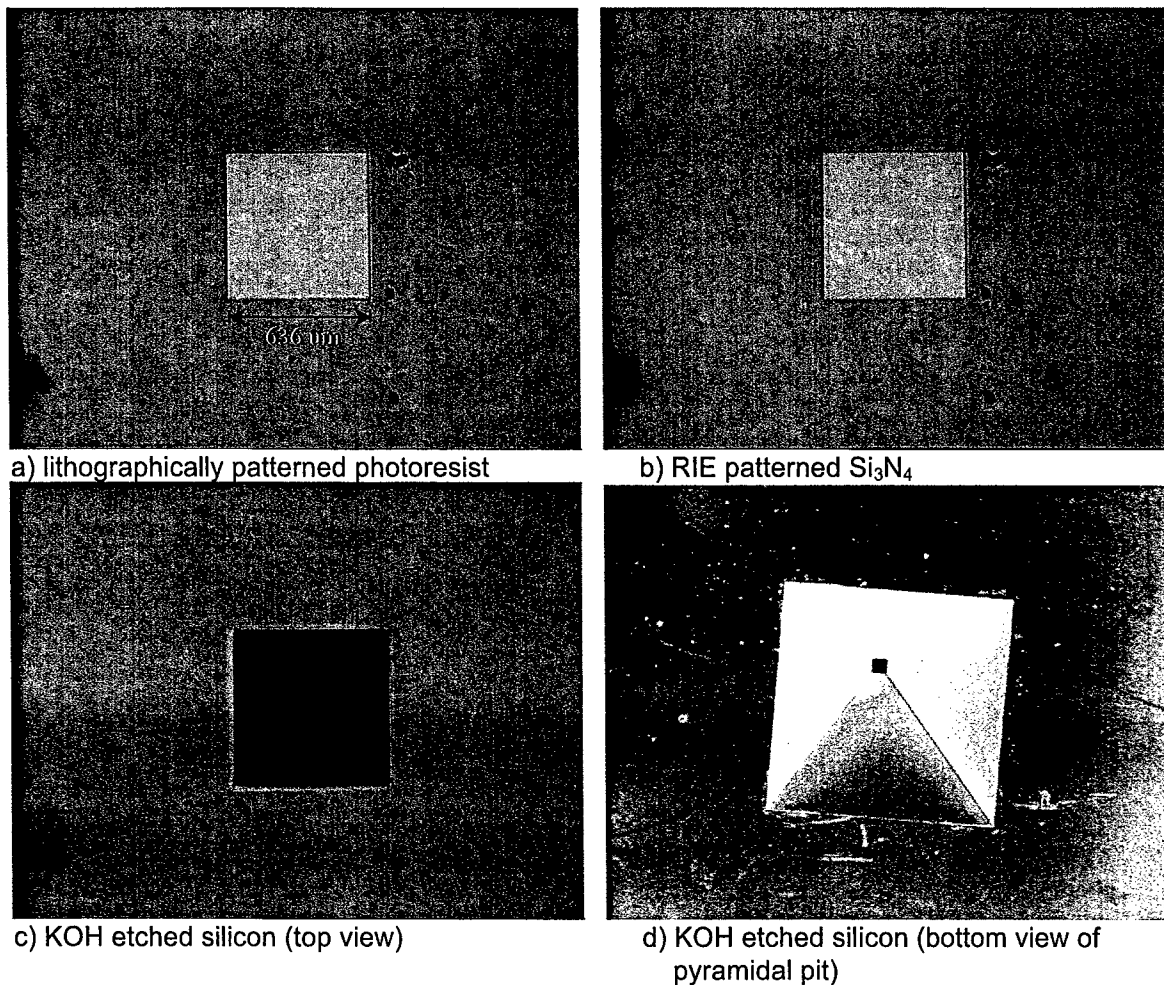d) KOH etched silicon (bottom view of pyramidal pit)

Figure 17. KOH bulk etched emitter chamber.

(Figure 17c and d).

Nozzle process recipe

Photoresist on the front side of the DSP wafer was lithographically patterned using a reverse imaging Karl Suss mask aligner to precisely center the emitter nozzle mask on top of the bulk etched chamber (Figure 18a). After development of the photoresist, nickel was vapor deposited over the surface. Lift-off in an acetone ultrasonic bath transferred the pattern to the nickel; a resistive mask to reactive ion etch. The exposed Si_3N_4 layer was removed in a CF_4/O_2 plasma RIE. Then, the nozzle was deep-etched using SF_6 RIE. The photo (Figure 18b) confirms our

15

precise alignment and successful etch to the chamber below.

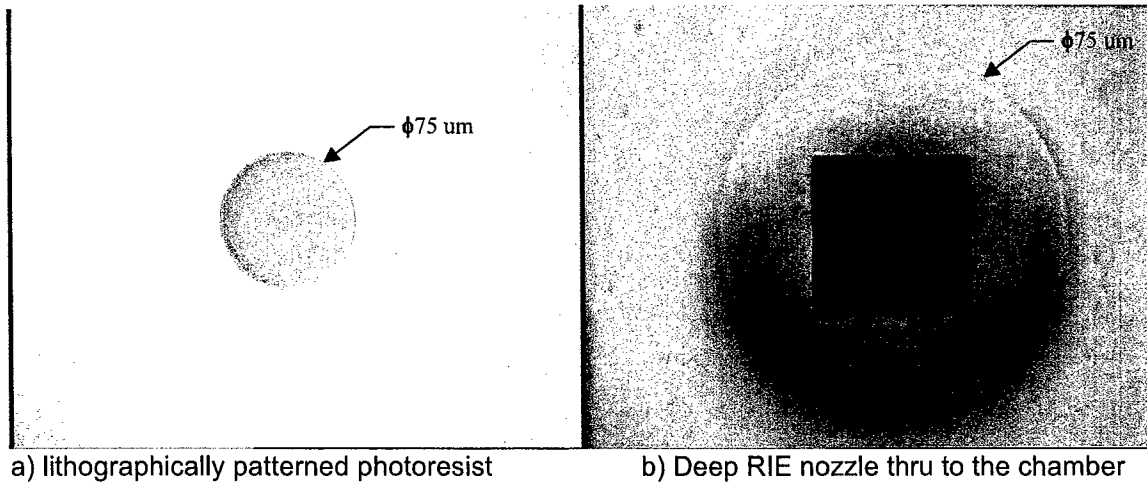| a) lithographically patterned photoresist | b) Deep RIE nozzle thru to the chamber |

Figure 18. Micro fabricated emitter nozzle by Deep RIE

TDA Research identified the Plasma Therm model 540 SF_6 plasma RIE processing parameters to rapidly and preferentially etch silicon. First, we cleaned the wafers using a 5 minute acetone bath in the ultrasonic cleaner followed by 5 minutes in an oxygen plasma. The oxygen plasma effectively cleaned organic materials from the surface. RIE power was systematically varied to study the effect on etch rate. Pre- and post-etch measurements were made of the silicon chip surface with a Dektac 3030 profilometer. Twenty minute etch times provided data with about 10% uncertainty in etch rate.

The silicon etch rate and selectivity were greatest with the chips placed directly onto the water-cooled aluminum surface. The highest etch rate was achieved at a 500W power setting with minimal degradation of the nickel mask (see Figure 19). A 2000Å thick nickel mask permitted etch depths to about 50 μm in 30 minutes.
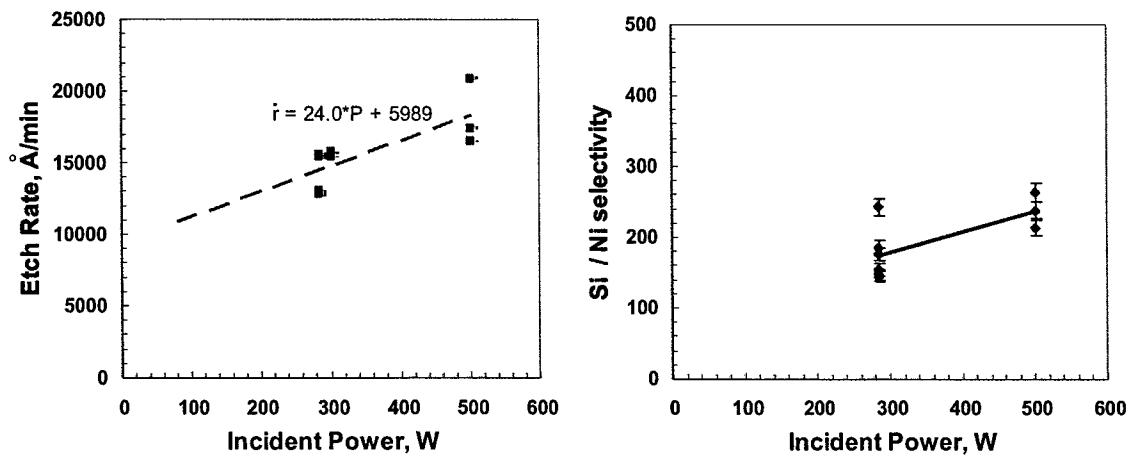

Figure 19. SF_6/O_2 RIE results at 80 mTorr, 5.0 sccm SF_6 and 0.5 sccm O_2. Samples were placed on the water-cooled aluminum plate.

16

Processing details are given below to etch the nozzle from the front side of the DSP wafer through to the chamber using RIE.

1) Piranha clean.
2) Spin coat hexamethyldisilazane (HMDS) primer for 40 sec at 4000rpm to improve adhesion. Next, spin coat Futurrex NR7-1500PY negative photoresist (PR) for 40 sec at 4000rpm. Then, pre-bake for 1 minute at 150°C on a vacuum hot plate.


spun-on PR
DSP wafer

3) Optional step: Pattern the wafer for thick outer edge removal using process steps 6-8 below. A special mask will be required for this purpose. Thus, the remaining PR is flat resulting in improved surface contact and feature resolution for lithography of the MEMS devices.
4) UV Lithography: mask align using a Karl Suss MJB3 and expose the wafer to UV light for ~25 to 30 seconds.
5) Post bake at 100°C for 1 minute on a vacuum hot plate.
6) Spray Futurrex RD6 developer onto the front side of the wafer for 5-6 seconds, while spinning at 800rpm. Watch for PR to wash off (reddish colors spin off and then the wafer looks clear). A second or two of over-development is OK. Apply de-ionized water for 20 sec to quench development and thoroughly rinse the wafer. Spin dry at 3000rpm.

patterned PR
DSP wafer
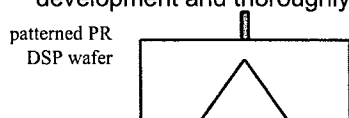
Note: the exposed PR is removed.

7) Use March III oxygen RIE to perform a 'de-scum' process for 10 seconds, which fully cleans the exposed oxide surface. Additional exposure may be required.
8) Vapor deposit 0.2um of nickel onto the wafer surface. Note: About 200Å of chromium is deposited first to improve adhesion of nickel to silicon.

vapor deposited nickel
patterned PR
DSP wafer
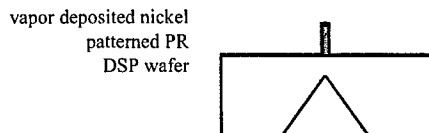
9) Immerse in acetone in ultrasonic cleaner to lift-off unwanted Ni and pattern the wafer.

patterned nickel
DSP wafer

10) SF$_6$ RIE etch through the wafer.

patterned nickel
micromachined
DSP wafer

11) Use etchant on hot plate at 50°C to remove the Ni mask and then Piranha clean.

micromachined
DSP wafer

Figure 20. Nozzle process recipe: UV lithography with negative PR followed by reactive ion etch.

17

4.3.2 Electrical components

Once all fluidic passages have been etched into the chip, it is cleaned and thermally oxidized to provide an insulating barrier between addressable emitter electrodes. Silicon oxide grown by thermal oxidation can withstand potentials as high as 1kV across a thickness of 1 μm, although Paine, et al. [2] have shown that flaws in the dielectric layer cause early voltage breakdown. These flaws were caused by microscopic contamination on the wafer surface that prevents oxidation immediately under the contaminant. Since we can only grow dielectric layers up to about 3 μm with this process, we used Teflon films for the dielectric between the emitter and extraction electrodes. These are commercially available from Dupont starting at ½ mil thickness and have 6500 V/mil breakdown voltage; more than enough to withstand the voltage needed to initiate Taylor cone extraction.

To make electrical wire traces and electrodes on top of the dielectric, we lithographically pattern a negative photoresist and then vapor deposit chromium and gold layers; total thickness of about 2000Å. Chromium forms an intermediate bond layer, since it adheres to silicon better than gold. The lift-off of the underlying sacrificial layer created the desired electrical circuit transmission line and electrode pattern. Thus, we can precisely define the emitter electrode separation in the array to avoid surface flashover, which occurs when the voltage gap between electrodes is short-circuited around the dielectric through open air or vacuum paths. Paine and Gabriel found that 50 μm of separation were sufficient for up to about 1500V [2].

Electrode process recipe

The following process details were needed to form the emitter and extraction electrodes, traces and wire bond pads on the front side of the DSP wafers (for example, see Figure 21). In the figure we show a lithographically patterned nickel electrode after the lift-off process. This demonstration showed that our line widths were sufficient to produce crisp features.
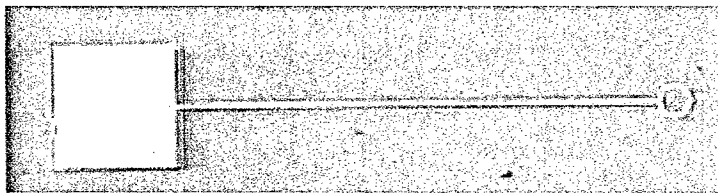

Figure 21. Emitter electrode, trace and wire bond pad.

18

1) **Piranha clean the wafer.**

2) Sputter a 5-10 μm thick oxide layer on of the dielectric to electrically isolate the wire traces.

3) Spin coat HMDS primer for 40 sec at 4000rpm. Then, spin coat Futurrex NR7-1500PY negative photoresist (PR) for 40 sec at 4000rpm. Then, pre-bake for 1 minute at 150°C on a vacuum hot plate.

spun-on PR
micromachined DSP wafer
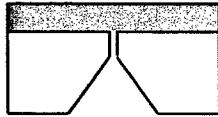
4) UV Lithography: mask align using a Karl Suss MJB3 and expose the wafer to UV light for ~25 to 30 seconds.

5) Post bake at 100°C for 1 minute on a vacuum hot plate.

6) Spray Futurrex RD6 developer onto the front side of the wafer for 5-6 seconds, while spinning at 800rpm. Watch for PR to wash off (reddish colors spin off and then the wafer looks clear). A second or two of over-development is OK. Apply de-ionized water for 20 sec to quench development and thoroughly rinse the wafer. Spin dry at 3000rpm.

patterned PR
micromachined DSP wafer
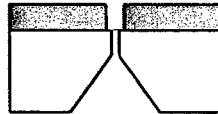
7) Vapor deposit about 1800Å of gold. Note: As was done for nickel vapor deposition, about 200Å of chromium is deposited first to improve adhesion of gold to silicon.

vapor deposited gold
patterned PR
micromachined DSP wafer

8) Immerse in acetone to lift-off unwanted gold and pattern the wafer.
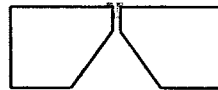
micromachined DSP wafer
w/ base electrode

Figure 22. Emitter electrode process recipe.

4.3.3 Thruster Component Alignment

In Phase I we used a micro stage bench to align thruster components during assembly. In Figure 23 we show a propellant delivery line aligned with a micro fabricated colloid emitter chip. Once positioned, we used two-part epoxy to bond the parts in place.

Fouling was problematic during assembly, so a wire was inserted through the pieces until the epoxy cured. It was then removed leaving an open flow path. Fouled passages will be much less likely to occur once we replace the adhesives with silicon-to-silicon diffusion bonds.

4.4 Design Validation Tests

In Phase I we conducted electrical and fluid flow tests to verify the emitter design and assembly procedure; the dielectric could withstand the high voltages needed for emitter actuation. We assembled a prototype MEMS colloid emitter that was installed in our test rig. As already mentioned, the emitter electrode was inadvertently blown off during assembly and thus did not produce an electrospray from the flowing propellant.
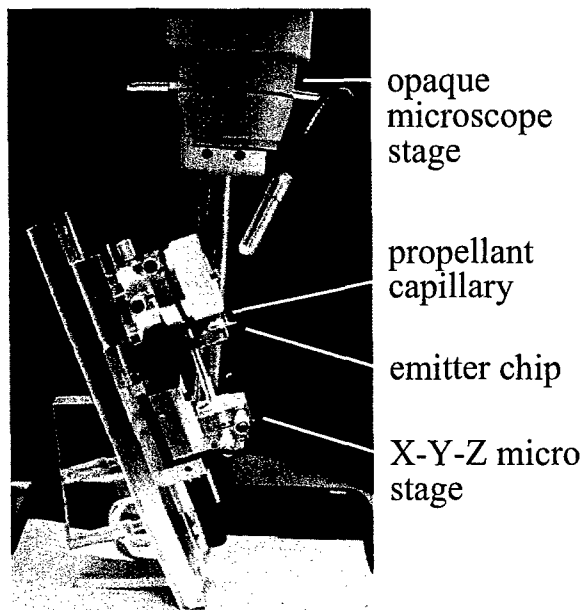

opaque microscope stage

propellant capillary

emitter chip

X-Y-Z micro stage

Figure 23. Micro stage assembly setup.

Voltage Breakdown

Voltage breakdown tests showed that 2 mil thick Teflon film can easily withstand more than 3000V. Further, we plan to have about 200 μm separation between our electrodes, which provides an additional margin of 950V in vacuum.

Colloid Emitter

The liquid propellant delivery system (Figure 24 and Figure 25) used a Harvard Apparatus Model 11 infuse / withdraw syringe pump (E-1) to precisely deliver very low propellant flow. The nominal flow rate of a single emitter will be about 2.4×10^{-4} mm^3/s for highly conductive propellants to as much as 1.9×10^{-2} mm^3/s for low conductance propellants. We can also visually confirm flow using a fused silica capillary bubble meter that has approximately 12% uncertainty for 30 second tests. Gaseous nitrogen provides the bubble source to the meter, which when inserted into the propellant stream (V-5) is tracked through a metered capillary (FM-1) using a video camera. We used tri-butyl phosphate doped with the ionic liquid 1-ethyl-3-methylimidazolium bis(trifluoromethylsulfonyl) imide (Strem Chemicals 07-0579) for our propellant. [7,8]

20

Figure 24. Propellant delivery and metering system.
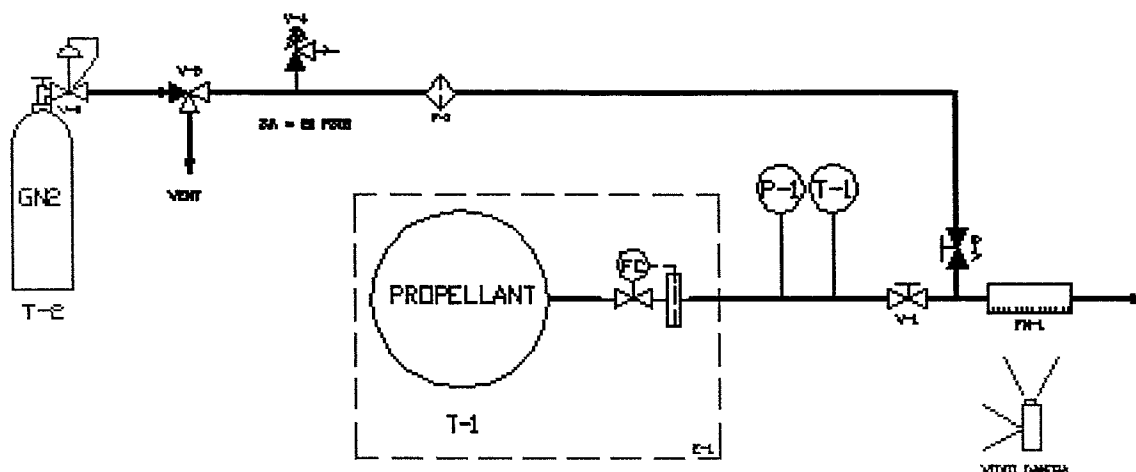
Component List:

E-1		infuse / withdraw micro syringe pump
T-1		ionic liquid propellant storage
T-2		gaseous nitrogen cylinder
V-1		propellant microvalve
V-2		gas cylinder pressure regulator
V-3		pressurization / vent 3-way valve
V-4		over-pressure relief valve
V-5		bubble insertion microvalve
F-1		0.1um filter
FM-1		bubble flow meter

The MEMS colloid emitter assembly was mounted onto an optical bench with three-axis positioning of the extraction electrode. Initially, we conducted validation tests using a 30 gauge Hamilton needle for the emitter electrode. Electrospray operation was confirmed for a tributyl phosphate propellant doped with 1.5% weight percent EMI-Im. The nominal electric field strength to initiate Taylor cone formation was about 1.5 V/µm at a 70 µL/hr flow rate (Figure 26a). We also demonstrated that the ion emission mode of operation could be achieved at a reduced flow condition (Figure 26b).
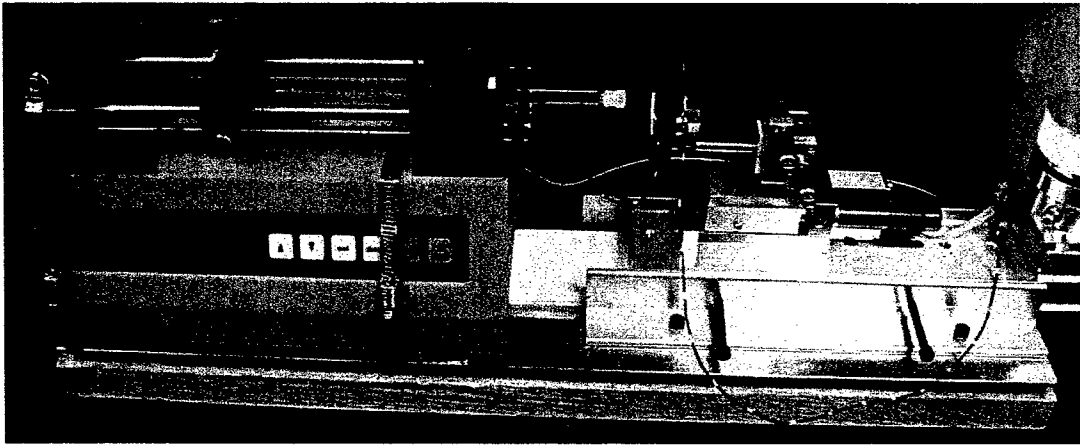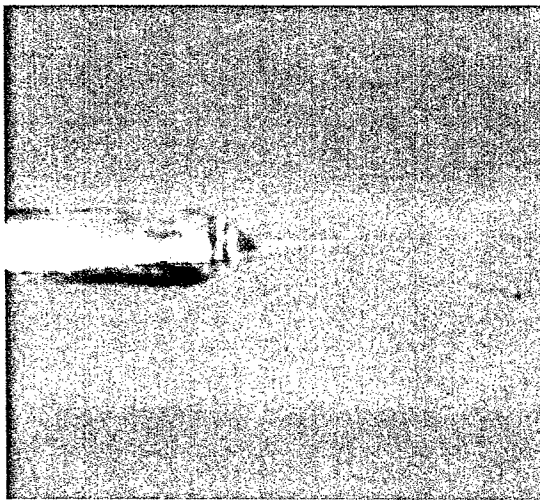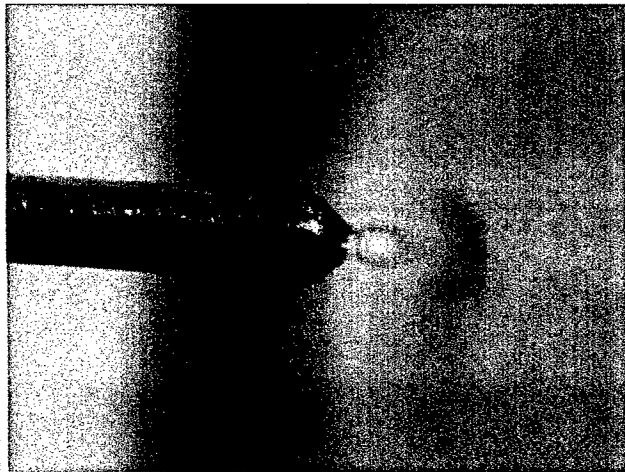
21

Figure 25. Colloid emitter laboratory setup.

a) electrospray mode   b) ion emission mode

Figure 26. Needle emitter operation.

Once validation tests were completed, a MEMS colloid emitter was installed and tested (Figure 27). The emitter had a 40 µm x 40 µm flow orifice just upstream of the 75 µm-diameter exit nozzle. A 10-µm-wide trace ran power to the 125-µm-OD annular electrode. Unfortunately, the emitter electrode was blown off while clearing a fouled flow passage, so MEMS colloid emitter operation could not be demonstrated. By hooking up power directly to the propellant feed line attached to the semi-conducting silicon substrate we were able to begin forming a cone, but this power connection changed the electrode geometry and substantially lowered the field strength. As a result, the local electric field was not strong enough at the emitter nozzle to generate an electrospray. This result was in line with our analytical predictions. In our future work we will need to coat the emitter electrode with a protective barrier layer to better withstand the handling, assembly and test environments that may be encountered.

Colloid emitter assembly and packaging will be a significant part of our Phase II effort. We will investigate Dow Corning Cyclotene™ and silicon dioxide as protective layers. The

22

microelectronics industry regularly uses Cyclotene™ as a protective topcoat and dielectric on circuit boards. It is easily applied by spin-coating, but compatibility with ionic liquids will need to be shown for use in our application. Alternatively, silicon dioxide layers can be sputtered onto the surface at low temperature to fully cover and protect the microelectronics.

Figure 27. MEMS colloid emitter.

5. Conclusion

In Phase I we designed a single MEMS colloid emitter that can be readily extended to a multi-emitter array. The annular electrodes proposed by TDA and UC-Boulder have high local electric field strength at the nozzle to reduce the voltage needed to activate the electrospray. We also designed a fluidic valve to passively meter flow to each emitter in the array. Detailed micro fabrication process recipes were developed and proven by actually building single emitters. A laboratory test rig has been built, validation tests were conducted using a conventional colloid capillary emitter and tests were attempted using a single MEMS colloid emitter.
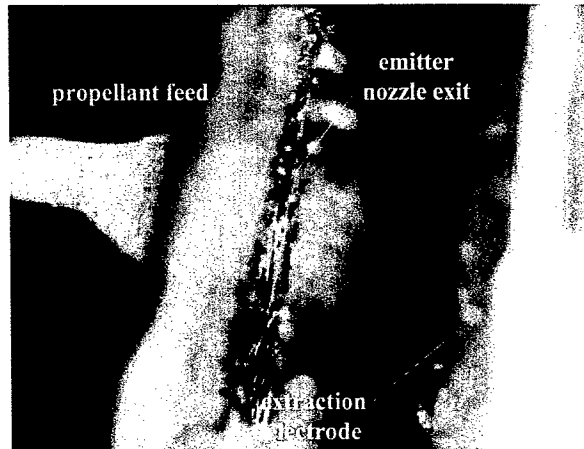
We continue to be excited by our MEMS colloid emitter technology, since it has several advantages over other approaches:

- **Annular emitter electrodes** – The annular emitter electrode design doubles the electric field strength in comparison to a full base electrode and thus, lowers the voltage needed to activate the electrospray. It can be micro machined using lithography and vapor deposition processes.
- **High voltage dielectrics** – Teflon films will be used during colloid emitter development to reduce risk. In a parallel task, we will develop and evaluate high quality sputtered silicon dioxide layers based on recent work at the University of Colorado MRTL. Using their equipment and sputter process we can create layers up to 10 μm thick; more than enough for high voltage actuation to 5 kV.
- **Integral flow control** – Passive fluidic valves meter propellant to each emitter in the array. Therefore, we expect the flows to be balanced during electrospray extraction from an array.
- **Micro machineable** – The proposed MEMS colloid multi-emitter can be readily fabricated using the processes defined in our Phase I Results section. Using these processes we expect to build addressable two-dimensional arrays in Phase II.

6. Relevant Publications

John Daily and James Nabity, "Electrostatic Modeling for MEMS Based Colloid Emitter Arrays," to be presented at the 41st AIAA/ASME/SAE/ASEE Joint Propulsion Conference & Exhibit, Tucson, AZ, July 2005.

John Daily and James Nabity, "Molecular Dynamics Simulation of Ion Emission from Nanodroplets of Ionic Liquid," to be presented at the 24th annual AAAR Conference, Austin, TX, October 2005.

7. New Discoveries, Inventions or Patent Disclosures

A patent disclosure will be prepared to describe our surface micromachined electrode design that has 2X the local field strength at the emitter nozzle as compared to a full base electrode.

8. References

1. Paine, M., and S. Gabriel, "A Micro-fabricated Colloidal Thruster Array," AIAA Paper 2001-3329 (2001).

2. Paine, M.D., S. Gabriel, C.G.J. Schabmueller and A.G.R. Evans, "Realization of Very High Voltage Electrode-Nozzle Systems for MEMS," submitted to Sensors and Actuators A Physical for publication (2004).

3. Krishnan, G., J. W. Daily and J. Nabity, "Simulation of an Electrostatically Driven Microinjector," 42nd AIAA Aerospace Sciences Meeting and Exhibit, Paper Number 2004-0305 (2004).

4. Nabity, J., G. Balducci and J.W. Daily, "Electrostatically Actuated Fuel Atomizer Design for the Pulse Detonation Engine," 39th AIAA/ASME/SAE/ASEE Joint Propulsion Conference and Exhibit, Paper Number 2003-4821 (2003).

5. J. Nabity and J. Daily, "A MEMS Fuel Atomizer for Advanced Engines," AIAA 2004-6711 presented at the CANEUS 2004—Conference on Micro-Nano-Technologies, 1-5 November 2004, Monterey, CA.

6. Mueller, J, "Thruster Options for Microspacecraft: A Review and Evaluation of Existing Hardware and Emerging Technologies," AIAA Paper 97-3053 (1997).

7. McEwen, A. B., Ngo, H. L., LeCompte, K., and Goldman, J. L., "Electrochemical Properties of Imidazolium Salt Electrolytes for Electrochemical Capacitor Applications," Journal of the Electrochemical Society, Vol. 146, No. 5, 1999, pp. 1687–1695.

8. M. Gamero-Castaño & V. Hruby, "Electric measurements of charged sprays emitted by cone-jets", Journal of Fluid Mechanics, 459, 245-276 (2002).

9. Distribution

Dr. Mitat Birkan
AFOSR/NA
4015 Wilson Blvd, Room 713
Arlington, VA 22203-1954